Available online at www.sciencedirect.com
ScienceDirect
Ceramics International 36 (2010) 1921–1927
CERAMICS INTERNATIONAL
www.elsevier.com/locate/ceramint

Microstructural features and electrical properties of copper oxide added potassium sodium niobate ceramics

Ebru Mensur Alkoy [a,*], Melih Papila [b]

[a] Faculty of Engineering, Maltepe University, Marmara Egitim Koyu, Maltepe, Istanbul 34857, Turkey
[b] Faculty of Engineering and Natural Sciences, Sabanci University, Tuzla, Istanbul 34956, Turkey

Received 5 November 2009; received in revised form 2 February 2010; accepted 22 March 2010
Available online 28 April 2010

Abstract

In this study, effects of 0.5, 1.0 and 1.5 mole% CuO addition on the properties of potassium sodium niobate $(K_{0.5}Na_{0.5})NbO_3$-KNN ceramics were investigated. Pure KNN and CuO-added KNN pellet samples were sintered at 1100 and 1090 °C for 4 h, respectively. Phase analysis showed that all samples crystallized in pure orthorhombic perovskite phase. Addition of 1.0 and 1.5 mole% CuO caused grain growth, densification and formation of a liquid phase at the grain boundaries. Curie temperature has shifted from 480 to 435 °C with increasing CuO ratio. The most remarkable characteristic of the hysteresis loops were the constricted nature of the 0.5 mole% CuO-added KNN's curve and the antiferroelectric-like appearance of the 1.5 mole% CuO-added KNN's curve. Piezoelectric properties of d_{33} = 120 pC/N, k_p = 0.27 and Q_m = 772 were obtained from the 1.5 mole% CuO-added KNN.

Keywords: A. Powders: solid state reaction; B. Microstructure-final; C. Ferroelectric properties; $(K,Na)NbO_3$

1. Introduction

Lead zirconate titanate (PZT) ceramics are high performance piezoelectric materials which are widely used in microelectronic and electronic devices as dielectric capacitors, ultrasonic or medical transducers, ultrasonic motors, actuators and sensors due to their superior dielectric, ferroelectric and piezoelectric properties [1]. However due to the toxicity of lead oxide and its high vapor pressure during the sintering process, the use of lead-based ceramics is restricted by law, and environmental and safety concerns regarding proper handling, disposal and recycling of lead containing materials have risen. So in recent years a great deal of effort have been spent on to develop lead-free piezoelectric materials with properties that are comparable to the properties of lead-based ones [2–4]. As a result, a number of studies on lead-free piezoelectric ceramics such as alkaline niobate, Bi-layered, $BaTiO_3$-based and tungsten bronze-type materials have been done.

Among these, potassium sodium niobate [$(K_{0.5}Na_{0.5})NbO_3$-(KNN)] is considered to be a promising candidate due to its comparable piezoelectric and ferroelectric properties to PZT and its high Curie temperature [5]. The densification of KNN is problematic but it can be improved by some methods such as addition of a sintering aid [3,4,6–10], modification of stoichiometry [2,11–15] and processing methods [16–19].

In this study, lead-free potassium sodium niobate $(K_{0.5}Na_{0.5})O_3$ (KNN) was prepared in bulk ceramic form. However, the final goal of our study is to fabricate lead-free KNN fibers. And due to the nature of the method used in drawing the fibers, which is explained elsewhere [20], processing methods such as hot pressing or spark plasma sintering cannot be used to improve densification behavior of KNN in this case. So, a chemical means, i.e. CuO sintering aid, was used to enhance densification. Thus, the main aim of the work presented in this paper is to prepare dense KNN using a sintering aid and investigation of the microstructural and electrical properties of these samples in detail.

2. Experimental

In this study, lead-free potassium sodium niobate $(K_{0.5}Na_{0.5})O_3$ (KNN) was produced by the conventional solid state reaction method from potassium carbonate, sodium

* Corresponding author. Tel.: +90 216 626 10 50; fax: +90 216 626 10 70.
E-mail address: ebrualkoy@maltepe.edu.tr (E.M. Alkoy).

0272-8842/$36.00
doi:10.1016/j.ceramint.2010.03.018

carbonate and niobium oxide powders (all chemicals were supplied from Alfa-Aesar). Powders were ball-milled in ethanol for 24 h with K:Na = 1:1 and this mixture was calcined at 900 °C for 4 h. After the calcination of KNN, copper oxide (CuO) was directly added to the KNN powder as a sintering aid in three different ratios (x = 0.5, 1.0 and 1.5 mole%). KNN and CuO powders were again ball-milled in ethanol for 12 h. The green KNN and KNN–CuO pellets were prepared by uniaxial dry pressing under 75 MPa. The CuO-added samples were sintered at 1090 °C and pure KNN samples were sintered at 1100 °C for 4 h. The sintered density of the ceramics was determined by the Archimedes method and Helium pycnometer. Silver–platinum electrode was applied to the parallel surfaces of the discs for electrical measurements and the electrode was fired at 850 °C for 30 min. The samples were poled by applying a DC electric field of 40 kV/cm for 30 min at 80 °C in silicon oil.

The microstructural features of samples were observed by Philips XL30 scanning electron microscope (SEM) (FEI, Hillsboro, OR, USA). The phase analysis was done by DMAX 2200 X-ray diffractometer (XRD) (Rigaku, Japan). Dielectric measurements were done using Hioki LCR meter (Hioki, Japan) and polarization vs. electric field hysteresis behavior was evaluated by Precision LC ferroelectric tester (Radiant Technologies, Inc., Albuquerque, NM, USA). HP 4194A Impedance Analyzer (Santa Clara, CA, USA) was used for impedance measurements.

3. Results

3.1. Phase analysis and microstructural features

Cu containing sintering aids in various forms have previously been used by other researchers to improve the densification behavior of the KNN ceramics. Matsubara et al. have tried novel $K_{5.4}Cu_{1.3}Ta_{10}O_{29}$ (KCT) [4] and $K_4CuNb_8O_{23}$ (KCN) [8] sintering aids, whereas Lin et al. [21] and Li et al. [22] directly added CuO to the calcined KNN powders. In all of these cases, Cu addition led to drastic changes in the structure and microstructure, as well as electrical properties of the KNN ceramics.

In the present study, the sintering aid was added to the calcined KNN powders in the form of CuO powder in various mole ratios. The XRD patterns of pure and CuO-added KNN pellets are shown in Fig. 1. These XRD results show that all samples crystallized in pure orthorhombic perovskite phase. A significant difference has not observed between the peaks of pure and CuO-added KNN.

The effects of CuO ratio on the microstructure were examined on ground, polished and thermally annealed sample surfaces by scanning electron microscopy (SEM). Fig. 2(a)–(d) show microstructures of the pure KNN pellets sintered at 1100 °C for 4 h and 0.5, 1.0, 1.5 mole% CuO-added KNN pellets sintered at 1090 °C for 4 h, respectively. A change of color on the sintered samples was observed as a function of CuO content. While the color of pure KNN sample was white, the color changed from a pale greenish gray to a dark gray with

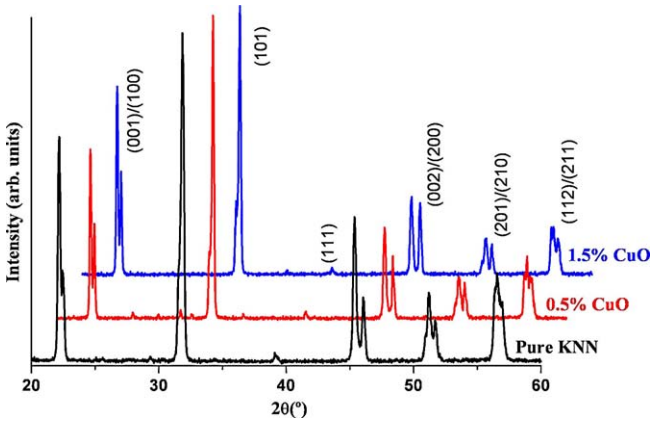

Fig. 1. X-ray diffraction patterns of KNN ceramics sintered at 1090 or 1100 °C for 4 h.

increasing amount of CuO. Increasing CuO ratio was found to cause drastic changes on the microstructure. In the case of undoped pure KNN (Fig. 2(a)), the ceramic was poorly densified with apparent presence of porosity. The density of this sample was determined to be 4.03 g/cm^3 which correspond to 89.3% of the theoretical density (4.51 g/cm^3) [4,8]. From Fig. 2(b), addition of 0.5 mole% CuO caused a densification of KNN while increasing the CuO content led to further densification and grain growth (Fig. 2(c)) for 1.0 mole%) and even formation of a liquid phase between the grains in the case of 1.5 mole% CuO addition (Fig. 2(d)). The density of KNN as a function of CuO addition in ratios of 0.5, 1.0 and 1.5 mole% were 4.19, 4.27 and 4.41 g/cm^3, respectively. These values correspond to 92.9, 94.7 and 97.8% of the theoretical density.

The densification of KNN ceramics was believed to proceed through formation of a liquid phase, as was also suggested in the literature [4,8]. A liquid phase contributes to sintering by accelerating particle redistribution due to enhanced atomic mobility and also enhances the final sample density via a high capillary force [23]. In the literature, observation of the liquid phase was achieved through quenching experiments [4,8]. However, in the present study, from Fig. 2(d), a liquid phase is clearly seen at the CuO-added KNN samples at the grain boundaries. However, this liquid phase requires further investigation with transmission electron microscopy and an electron diffraction study to clearly identify its chemical and structural nature.

The general grain growth observed in CuO-added KNN is also believed to be a result of the liquid phase observed at the grain boundaries. From Fig. 2(a), pure KNN was found to have a bimodal grain size distribution with some of the grains having a grain size of <1 μm and others with sizes on the order of 5 μm or more. A similar microstructure was observed in pure KNN by Zhen and Li [23] as a result of increasing sintering temperature. Addition of a small amount of CuO (0.5 mole%) was found to led to a grain coarsening (Fig. 2(b)) (average grain size of 2.3 μm) and further crystallization. Additional increase in the CuO content (1.0 and 1.5 mole%) led to a more severe growth of smaller grains and a general homogenization of grain

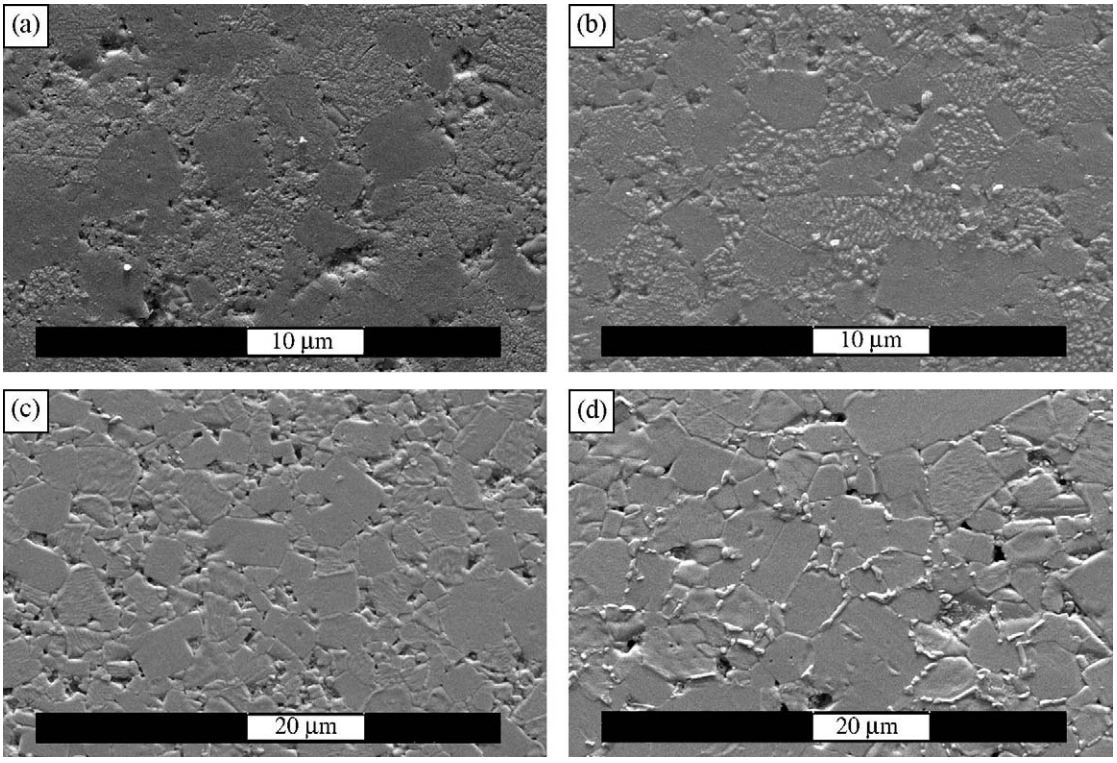

Fig. 2. Scanning electron micrographs of (a) pure KNN sintered at 1100 °C-4 h, (b) 0.5 mole% CuO-added KNN sintered at 1090 °C-4 h, (c) 1.0 mole% CuO-added KNN sintered at 1090 °C-4 h and (d) 1.5 mole% CuO-added KNN sintered at 1090 °C-4 h.

sizes (Fig. 2(c) and (d)) (average grain size of 3.75 μm for 1.0 mole% CuO-added KNN and 6.5 μm for 1.5 mole% CuO-added KNN). A similar trend was also observed by other researchers [24]. Since pure KNN has a bimodal grain size distribution, this drastic grain growth process is believed to be a result of Ostwald ripening process where large grains (or particles) grow at the expense of finer grains (or particles) in a system with a distribution of sizes. Further growth of large grains is driven by the difference in surface free energies between the advancing plane of large grains and the fine matrix grains. The presence of a liquid phase in especially the 1.5 mole%CuO-added KNN facilitates and accelerates the kinetics of this process. This is understandable considering the fact that the rate of diffusion by solid state processes ranges from 10^{-9} to 10^{-12} cm^2/s, whereas in the liquid it ranges from 10^{-4} to 10^{-5} cm^2/s [25]. Thus, a liquid forming sintering aid such as CuO has a very critical role to fabricate dense KNN ceramics with a uniform and narrow grain size distribution compared to pure KNN.

3.2. Dielectric and ferroelectric properties

In the investigation of the electrical properties 1.5 mole% CuO-added ceramics were taken into consideration and compared with the pure and 0.5 mole% CuO-added KNN.

The effect of CuO on electrical properties would be several folds and should be listed here before presenting and discussing the results of the electrical measurements. The main effect of CuO is the formation of a liquid phase as a sintering aid, and thereby, enhancing the sintering efficiency, increasing the density of the KNN ceramics and decreasing the porosity. This is clearly visible from Fig. 2 and from the density measurements, and discussed in detail in the preceding section. In the literature, increased density of KNN has been reported [4,8] to yield better electrical properties, i.e. higher values of P_r, Q_m, etc. Another effect of CuO is on the grain size of KNN, as seen in Fig. 2, where increasing CuO content led to a drastic increase in the grain size and a shift from bimodal grain size distribution to a more narrow and uniform one. From a microstructural point of view, smaller grains with submicron sizes, such as those of pure KNN in Fig. 2(a), may have a higher domain wall density, which in turn results in higher extrinsic contribution on the electrical properties [26]. But on the other hand, smaller grains may lead to higher stresses inside the grain, absence of 90° domain walls and decreased domain mobility [26,27]. Therefore, the effect of grain size on the electrical properties is of a complex nature with competing effects. It also requires a detailed microstructural investigation of the domain structure in polycrystalline samples. A second microstructural effect of CuO is the formation of a secondary grain boundary phase, which is especially more pronounced and clearly identifiable in 1.5 mole% CuO content (Fig. 2(d)). Depending on the extent, continuity and the electrical properties of this secondary phase, its effect might be significant. If, particularly, the conductivity of this phase is higher than the KNN grains, then its effect might be deleterious. Finally, the CuO-added to KNN would not only act as a sintering aid, but some of the Cu^{2+} ions will enter into the ABO_3

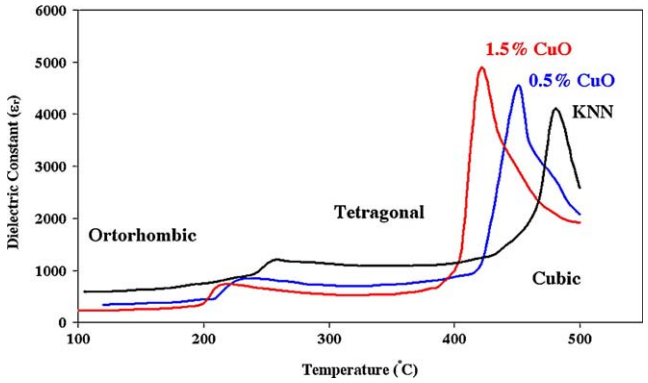

Fig. 3. Temperature dependent dielectric constant of KNN ceramics.

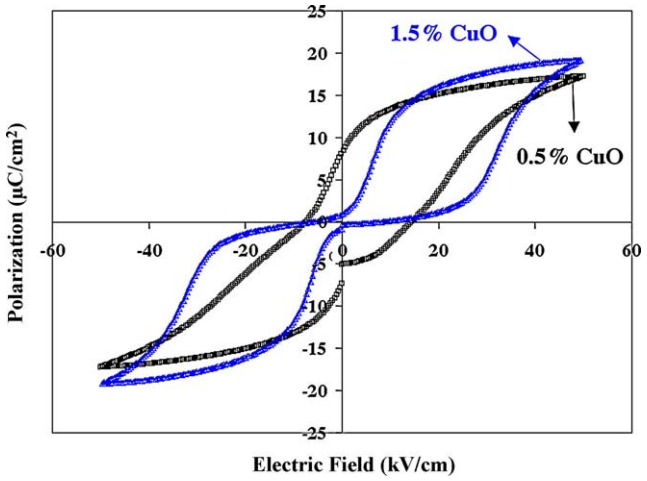

Fig. 4. Polarization vs. electric field hysteresis loops of KNN ceramics sintered at 1090 °C for 4 h before DC poling.

perovskite structure. Taking Shannon's [28] ionic radii into consideration, Cu^{2+} will occupy B site and replace Nb^{5+} as an acceptor dopant and produces positively charged oxygen vacancies to maintain the charge neutrality according to the following defect equation [4,22,24].

$$Nb_{Nb} + \frac{3}{2}O_O + CuO \rightarrow Cu''''_{Nb} + \frac{1}{2}Nb_2O_5 + \frac{3}{2}V_O^{\bullet\bullet} \quad (1)$$

The Cu^{2+} ion accommodated at the Nb^{5+} site and the oxygen vacancy may form a defect dipole that can provide a domain pinning effect transforming KNN into a hard piezoelectric ceramic [22,24]. The electrical properties of CuO-added KNN ceramics will be presented and tried to be explained in the light of the preceding discussion on the possible and competing effects of CuO addition on KNN.

The temperature dependence of dielectric constant of pure and CuO-added KNN ceramics at 100 kHz from 100 to 500 °C is shown in Fig. 3. All samples showed two peaks; one above 200 °C and another above 400 °C which corresponds to the orthorhombic–tetragonal phase transition (T_{ot}) and tetragonal-cubic phase transition (Curie temperature-T_c), respectively. It is clearly seen that, T_c has shifted from 480 to 435 °C and T_{ot} from 255 to 220 °C with increasing CuO ratio. The peaks of all three ceramics at the Curie temperature are sharp, indicating that the ceramics are showing a normal ferroelectric behavior and that CuO addition does not change this character [29]. The low temperature dielectric constant of KNN in the orthorhombic phase was also found to decrease as a function of increasing CuO content. This is thought to be a due to a shift in the behavior of KNN towards a hard piezoelectric material by increasing pinning of domains and lower contribution from to the domain wall motion to the low voltage dielectric properties with increasing CuO content, as explained above.

In Fig. 4, polarization vs. electric field hysteresis (*P–E*) loops of CuO-added KNN samples are given. The *P–E* loops of pure KNN samples could not be included in this figure because this measurement could not be taken from pure KNN samples due to the leakage current of the insufficiently densified samples, similar to the observation of Matsubara et al. [4] The most striking feature of these *P–E* loops is the constricted nature of the 0.5 mole% CuO-added KNN's curve and the antiferroelectric-like appearance of the 1.5 mole% CuO-added KNN's curve.

In the literature similar constricted and antiferroelectric-like double hysteresis curves were also observed in CuO-added KNN ceramics by Chan's [21,29] and Tsurumi's [22] groups. Double *P–E* hysteresis curves have also been observed in aged $Pb_\lambda Ca_{1-\lambda}TiO_3$ [30] and Mn-doped $BaTiO_3$ [31]. The observation of double *P–E* curves in the aged ferroelectric titanates has been attributed to the acceptor doping and formation of defect dipoles. In the case of Cu-doped KNN, the point defects Cu''''_{Nb} and $V_O^{\bullet\bullet}$ created in the KNN perovskite lattice were cited as the reason for the observation of the double hysteresis loops [21,22,29,32]. Tsurumi's [22] group suggests that some of these point defects releases electrons and holes which develops a space charge. After a long aging, these space charges were speculated [22] to accumulate at the domain boundaries creating an internal electric field (E_i) along the direction of the spontaneous polarization (P_s). During the *P–E* measurements this E_i was reported [22] to force the polarization to switch back to its original orientation when the externally applied field is removed, thus, reducing the remnant polarization (P_r) to zero. Chan's [32] work, on the other hand, states that the requirement of aging process to observe the double hysteresis loop depends on the temperature of the orthorhombic-tetragonal transition. In their work, it was reported that if the temperature is high (~206 °C) [32], then the oxygen vacancies can migrate during the crystal transformation and settle in a distribution with the same symmetry as the crystal after the transformation. As a result, defect dipoles ($Cu''''_{Nb} - V_O^{\bullet\bullet}$) along the polarization direction are suggested [32] to form and provide restoring forces to reverse the switched polarizations, and thus, producing a double hysteresis (*P–E*) loop. Aging was cited as a requirement if the transition temperature is low (~175 °C) [32], where the defect symmetry may not correct to the crystal symmetry completely after the fabrication process due to the low migration rate of the defect dipoles, and thus the P–E loop is not constricted significantly. However, after aging, these ceramics were also reported [32] to exhibit the double hysteresis loops.

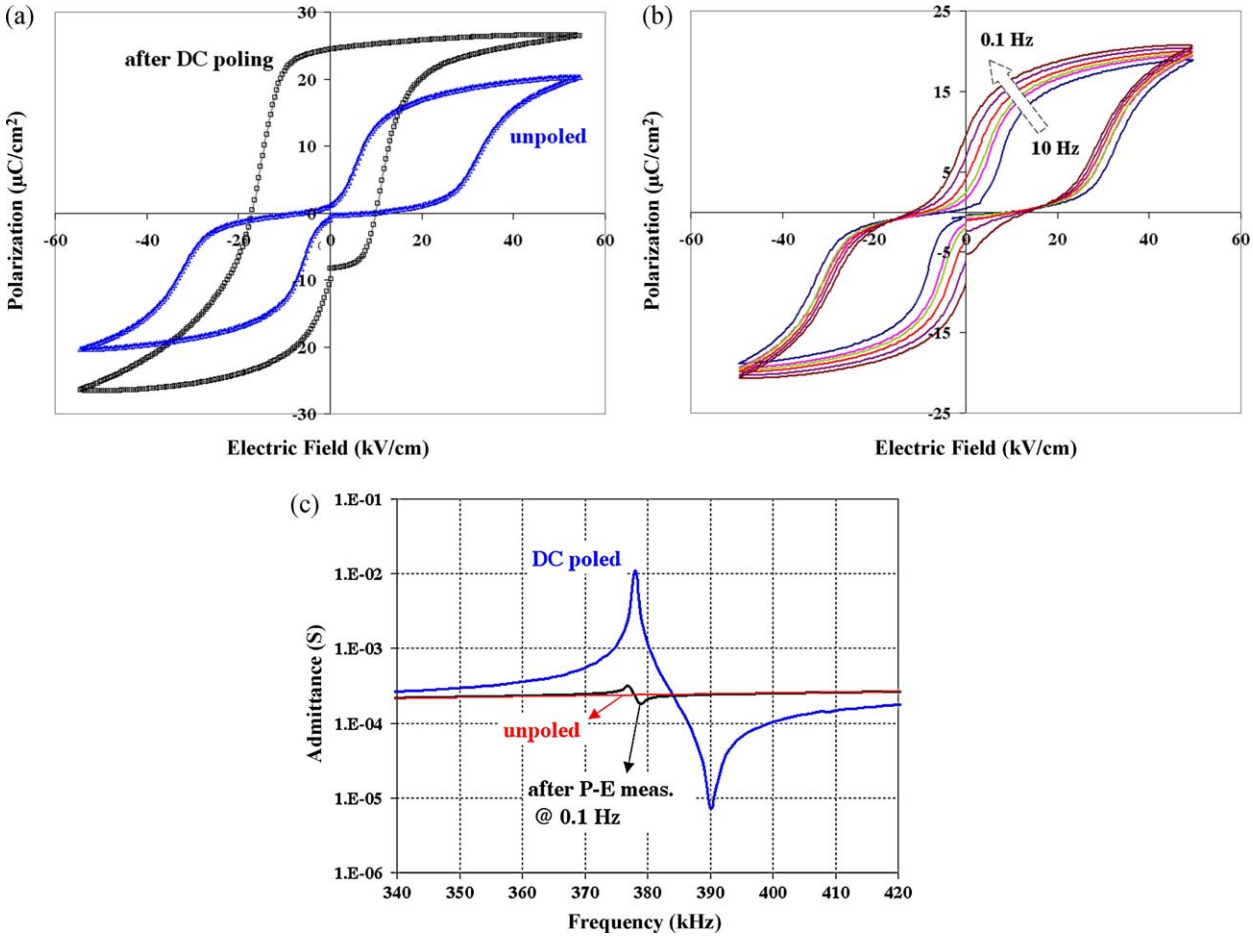

Fig. 5. (a) Polarization vs. electric field hysteresis loops of 1.5 mole% CuO-added KNN ceramics sintered at 1090 °C for 4 h before and after DC poling, (b) polarization vs. electric field hysteresis loops of 1.5 mole% CuO-added KNN ceramics sintered at 1090 °C for 4 h before DC poling and (c) admittance vs. frequency spectra of 1.5 mole% CuO-added KNN ceramics sintered at 1090 °C for 4 h.

The constricted and antiferroelectric-like double hysteresis *P–E* loops observed in our study will be discussed in the light of these mechanisms from literature [21,22,29,32] presented in the previous paragraph. In our study, the transition temperatures T_c and T_{ot} are rather high (from Fig. 3, 435–480 and 220–255 °C, respectively) and the double hysteresis behavior was observed right after firing above the Curie temperature without any aging process. Therefore, aging was not believed to be involved in the case of this study. The *P–E* behavior was investigated further. Fig. 5(a) compares the *P–E* loops of unpoled and DC poled samples. Applying DC poling causes the double hysteresis behavior to disappear and resulted in a normal ferroelectric *P–E* loop. The asymmetry observed in the loops is due to the imprint developed as a result of DC poling. The stability of the defect dipoles at room temperature were investigated by taking the *P–E* measurements at different frequencies from 10 Hz down to 0.1 Hz. From Fig. 5(b), as the frequency decreases, low field region of the double *P–E* loop gradually swells and starts to resemble a normal, single but constricted *P–E* loop characteristic of hard piezoelectric ceramics. From this observation, it can be concluded that if the switching period is long enough (e.g., 0.1 Hz), the vacancies will have enough time to migrate, allowing the defect dipoles to rotate with the electric field. As a result of this rotation, the restoring force decreases and the reversal of the switched polarization cannot be completed, leading to a single *P–E* loop.

The piezoelectric activity of the 1.5 mole% CuO-added KNN ceramics at various stages were investigated through admittance vs. frequency and piezoelectric charge coefficient (d_{33}) measurements and the results were correlated with the net polarization developing during the *P–E* measurements. From Fig. 5(c), unpoled sample with double hysteresis loop and zero remnant polarization does not display any resonance behavior in the admittance spectrum, indicating no piezoelectric activity. The d_{33} coefficient of the sample at this stage was zero, as expected. The admittance spectra of the poled sample with a normal, single *P–E* loop, on the other hand, displays a clear and sharp resonance behavior, signature of a strong piezoelectric activity. The d_{33} coefficient of the sample at this stage was approximately 120 pC/N, accordingly. However, as discussed above, measuring the *P–E* hysteresis at low frequencies (0.1 Hz) led to a swelling of the *P–E* curve at low fields and development of a remnant polarization. In parallel with this development, the admittance spectrum of the sample at this

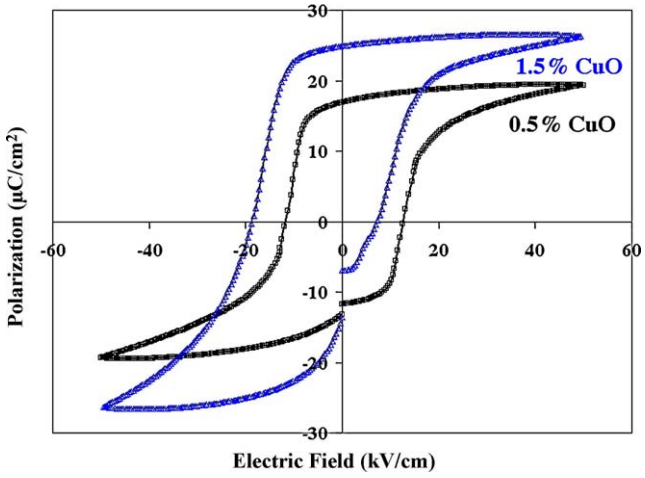

Fig. 6. Polarization vs. electric field hysteresis loops of KNN ceramics sintered at 1090 °C for 4 h after DC poling.

stage displays a small but visible resonance behavior, indicative of a weak piezoelectric activity. The d_{33} coefficient of the sample at this stage was supportive of this development and was measured as 60 pC/N.

The effect of increasing CuO content on the *P–E* hysteresis loops of CuO-added KNN ceramics after DC poling were compared in Fig. 6. From this figure, increasing CuO content was found to increase the remnant polarization of CuO-added KNN, whereas, the coercive field was found to remain unchanged. A similar increase of P_r with increasing Cu content was observed by Li et al. [22] and Matsubara et al. [8]. An explanation has not been offered in the literature for this observed increase. However, in our case, this increase is believed to be due to the increased density and grain size of the ceramics with increasing CuO content.

Finally, the mechanical quality factor (Q_m) and planar coupling coefficient (k_p) of CuO-added KNN samples have been investigated through admittance vs. frequency measurements. A high Q_m value is desirable for resonant piezoelectric devices to suppress heat generation during the operation of the device [8,22]. In the literature [8,22], the k_p and Q_m values of undoped KNN are reported to be 35–39 and 85–90%, respectively. The k_p and Q_m values were determined using the relationships [8]

$$\frac{1}{k_p^2} = 0.395\frac{f_r}{f_a - f_r} + 0.574 \quad (2)$$

$$Q_m = \frac{1}{2\pi f_r R_1 C_f\{1 - (f_r/f_a)^2\}} \quad (3)$$

where f_r: resonance frequency, f_a: antiresonance frequency, R_1: resonance impedance, C_f: capacitance at 1 kHz. From our measurements and using the relationships given above, the k_p values of 0.5 and 1.5 mole% CuO-added KNN ceramics were calculated as 28.4 and 26.6%, respectively. The Q_m values, on the other hand, were found to increase from 398 to 772 with the additions of 0.5 and 1.5 mole% CuO to the KNN. In the literature, increase in Q_m values was associated with an increase in elastic properties of the ceramic [4], i.e. the density and a hardening of piezoelectric properties [22,29]. From Fig. 2 and the results of density measurements, densification of KNN with increasing CuO content is obvious. Additionally, hardening of the piezoelectric properties due to domain pinning by the defect dipoles have been demonstrated through the constriction and, even, observation of double hysteresis behavior in the *P–E* loops. Thus, the increase in Q_m with the addition of CuO is justifiable. Additionally, from Eq. (3), Q_m is inversely proportional to the impedance and capacitance. The impedance at resonance of 0.5 and 1.5 mole% CuO-added KNN ceramics are 55 and 90 Ω, respectively. The capacitance, on the other hand, drops from 320 to 100 pF. Thus, the increase in Q_m can mostly be attributed to the decrease in the dielectric properties with increasing CuO addition.

4. Conclusion

The effect of CuO addition on both the microstructural and the electrical properties of the KNN ceramics were investigated in this study. A significant difference has not been observed between the XRD patterns of pure and CuO-added KNN. However, increasing CuO ratio was found to cause drastic changes on the microstructure. The main effect of CuO is the formation of a liquid phase at the grain boundaries as a sintering aid, and thereby, enhancing the sintering efficiency and increasing the density of the KNN ceramics. Especially, 1.0 and 1.5 mole% CuO caused grain growth, a narrowing of the grain size distribution, further densification and formation of a liquid phase at the grain boundaries. All samples showed two peaks in the temperature dependent dielectric measurements; the orthorhombic–tetragonal phase transition (T_{ot}) and tetragonal–cubic phase transition (Curie temperature-T_c). It is observed that, T_c has shifted from 480 to 435 °C and T_{ot} from 255 to 220 °C with increasing CuO ratio. The peaks of pure and added KNN ceramics at the Curie temperature are sharp, indicating that the ceramics are showing a normal ferroelectric behavior and that CuO addition does not change this character. The low temperature dielectric constant of KNN in the orthorhombic phase was also found to decrease as a function of increasing CuO content. This is thought to be a due to increasing pinning of domains and lower contribution from to the domain wall motion to the low voltage dielectric properties with increasing CuO content. The most striking feature of the polarization vs. electric field hysteresis loops are the constricted nature of the 0.5 mole% CuO-added KNN's curve and the antiferroelectric-like appearance of the 1.5 mole% CuO-added KNN's curve. This was believed to be due to domain stabilizing effect of the defect dipoles that were formed as a result of Cu^{2+} cations replacing Nb^{5+} and oxygen vacancies forming to balance the electroneutrality. The d_{33} coefficient of the 1.5 mole% CuO-added poled sample was approximately 120 pC/N. The Q_m value of KNN was found to increase from 398 to 772 with the additions of 0.5 and 1.5 mole% CuO to the KNN. In conclusion, dense KNN ceramics were obtained through CuO addition.

Acknowledgement

The authors wish to acknowledge the financial support of Turkish Academy of Sciences.

References

[1] G.H. Haertling, Ferroelectric ceramics: history and technology, J. Am Ceram. Soc. 82 (4) (1999) 797–818.
[2] Y. Saito, H. Takao, T. Tani, T. Nonoyama, K. Takatori, T. Homma, T. Nagaya, M. Nakamura, Lead-free piezoceramics, Nature 432 (2004) 84–87.
[3] N.M. Hagh, K. Kerman, B. Jadidian, A. Safari, Dielectric and piezoelectric properties of Cu^{2+}-doped alkali niobates, J. Eur. Ceram. Soc. 29 (11) (2009) 2325–2332.
[4] M. Matsubara, T. Yamaguchi, K. Kikuta, S. Hirano, Sintering and piezoelectric properties of potassium sodium niobate ceramics with newly developed sintering aid, Jpn. J. Appl. Phys. 44 (1A) (2005) 258–263.
[5] L. Egerton, D.M. Dillom, Piezoelectric and dielectric properties of ceramics in the system potassium–sodium niobate, J. Am. Ceram. Soc. 42 (9) (1959) 438–442.
[6] D. Lin, K.W. Kwok, H.L.W. Chan, Microstructure, dielectric and piezoelectric properties of $(K_{0.5}Na_{0.5})NbO_3$–$Ba(Ti_{0.95}Zr_{0.05})O_3$ lead-free ceramics with CuO sintering aid, Appl. Phys. A 88 (2007) 359–363.
[7] D. Lin, K.W. Kwok, H.L.W. Chan, Piezoelectric and ferroelectric properties of $K_xNa_{1-x}NbO_3$ lead-free ceramics with MnO_2 and CuO doping, J. Alloys Compd. 461 (2008) 273–278.
[8] M. Matsubara, T. Yamaguchi, K. Kikuta, S. Hirano, Sinterability and piezoelectric properties of (K,Na)NbO_3 ceramics with novel sintering aid, Jpn. J. Appl. Phys. 43 (10) (2004) 7159–7163.
[9] E. Li, H. Kakemato, S. Wada, T. Tsurumi, Influence of CuO on the structure and piezoelectric properties of the alkaline niobate-based lead-free ceramics, J. Am. Ceram. Soc. 90 (6) (2007) 1787–1791.
[10] S. Su, R. Zuo, X. Wang, L. Li, Sintering, microstructure and piezoelectric properties of CuO and SnO_2 co-modified sodium potassium niobate ceramics, Mater. Res. Bull. 45 (2) (2010) 124–128.
[11] E. Hollenstein, E. Davis, D. Damjanovic, N. Setter, Piezoelectric properties of Li- and Ta-modified $(K_{0.5}Na_{0.5})NbO_3$ ceramics, Appl. Phys. Lett. 87 (18) (2005) 182905–182908.
[12] K. Matsumoto, Y. Hiruma, H. Nagata, T. Takenaka, Electric-field-induced strain in Mn-doped $KNbO_3$ ferroelectric ceramics, Ceram. Int. 34 (2008) 787–791.
[13] Y. Guo, K. Kakimoto, H. Ohsato, Phase transitional behavior and piezoelectric properties of $(Na_{0.5}K_{0.5})NbO_3$–$LiNbO_3$ ceramics, Appl. Phys. Lett. 85 (18) (2004) 4121–4123.
[14] Y. Zhou, M. Guo, C. Zhang, M. Zhang, Hydrothermal synthesis and piezoelectric property of Ta-doping $K_{0.5}Na_{0.5}NbO_3$ lead-free piezoelectric ceramic, Ceram. Int. 35 (2009) 3253–3258.
[15] G. Jiao, H. Fan, L. Liu, W. Wang, Structure and piezoelectric properties of Cu-doped potassium sodium tantalate niobate ceramics, Mater. Lett. 61 (2007) 4185–4187.
[16] N.M. Hagh, B. Jadidian, A. Safari, Property-processing relationship in lead-free (K, Na, Li)NbO_3-solid solution system, J. Electroceram. 18 (2007) 339–346.
[17] R.E. Jeager, L. Egerton, Hot pressing of potassium-sodium niobates, J. Am. Ceram. Soc. 45 (5) (1962) 209–213.
[18] J. Li, Y. Zhen, B. Zhang, L. Zhang, K. Wang, Normal sintering of $(Na_{0.5}K_{0.5})NbO_3$-based lead-free piezoelectric ceramics, Ceram. Int. 34 (2008) 783–786.
[19] R. Chang, S. Chu, Y. Lin, C. Hong, Y. Wong, The effects of sintering temperature on the properties of $(Na_{0.5}K_{0.5})NbO_3$–$CaTiO_3$ based lead-free ceramics, Sens. Actuators A: Phys. 138 (2007) 355–360.
[20] S. Alkoy, H. Yanık, B. Yapar, Fabrication of lead zirconate titanate ceramic fibers by gelation of sodium alginate, Ceram. Int. 33 (2007) 389–394.
[21] D. Lin, K.W. Kwok, H.L.W. Chan, Double hysteresis loop in Cu-doped $K_{0.5}Na_{0.5}NbO_3$ lead-free piezoelectric ceramics, Appl. Phys. Lett. 90 (23) (2007) 232903–232906.
[22] E. Li, H. Kakemato, S. Wada, T. Tsurumi, Enhancement of Q_m by co-doping of Li and Cu to potassium sodium niobate lead-free ceramics, IEEE Trans. Ultrason. Ferroelectr. Freq. Control 55 (5) (2008) 980–987.
[23] Y. Zhen, J.F. Li, Abnormal grain growth and new core–shell structure in (K,Na)NbO_3-based lead-free piezoelectric ceramics, J. Am. Ceram. Soc. 90 (11) (2007) 3496–3502.
[24] H.Y. Park, J.Y. Choi, M.K. Choi, K.H. Cho, H.G. Lee, H.W. Kang, S. Nahm, Effect of CuO on the sintering temperature and piezoelectric properties of $(Na_{0.5}K_{0.5})NbO_3$ lead-free piezoelectric ceramics, J. Am. Ceram. Soc. 91 (7) (2008) 2374–2377.
[25] G.L. Messing, S. Trolier-McKinstry, E.M. Sabolsky, C. Duran, S. Kwon, B. Brahmaroutu, P. Park, H. Yilmaz, P.W. Rehrig, K.B. Eitel, E. Suvaci, M. Seabaugh, K.S. Oh, Templated grain growth of textured piezoelectric ceramics, Crit. Rev. Solid State Mater. Sci. 29 (2) (2004) 45–96.
[26] W. Cao, C.A. Randall, Grain size and domain size relations in bulk ceramic ferroelectric materials, J. Phys. Chem. Solids 57 (10) (1996) 1499–1505.
[27] D. Damjanovic, Ferroelectric, dielectric and piezoelectric properties of ferroelectric thin films and ceramics, Rep. Prog. Phys. 61 (1998) 1267–1324.
[28] R.D. Shannon, Revised effective ionic radii and systematic studies of interatomic distances in halides and chalcogenide, Acta Crystallogr. A32 (1976) 751–767.
[29] D. Lin, K.W. Kwok, H.L.W. Chan, Piezoelectric and ferroelectric properties of Cu-doped $K_{0.5}Na_{0.5}NbO_3$ lead-free ceramics, J. Phys. D: Appl. Phys. 41 (2008), 045401-045401-6.
[30] E. Sawaguchi, M.L. Charters, Aging and the double hysteresis loop of $Pb_\lambda Ca_{1-\lambda}TiO_3$ ceramics, J. Am. Ceram. Soc. 42 (4) (1959) 157–164.
[31] L.X. Zhang, X.B. Ren, Aging behavior in single-domain Mn-doped $BaTiO_3$ crystals: Implication for a unified microscopic explanation of ferroelectric aging, Phys. Rev. B 73 (9) (2006), 094121-094121-6.
[32] D. Lin, K.W. Kwok, H.L.W. Chan, Double hysteresis loop and aging effect in $K_{0.5}Na_{0.5}NbO_3$-$K_{5.4}Cu_{1.3}Ta_{10}O_9$ lead-free ceramics, J. Am. Ceram. Soc. 92 (6) (2009) 1362–1365.